

# Analysis of Electronic Threshold of PRAM Cell Operation

Young-Tae Kim, Keun-Ho Lee, Young-Kwan Park and Jeong-Taek Kong

CAE Team, Memory Division, Semiconductor Business, Samsung Electronics co., LTD.

San #16 Banwol-Ri, Taean-Eup, Hwasung-City, Gyeonggi-Do, 445-701, Korea (E-mail:rokmc.kim@samsung.com)

**Abstract** – In this paper, the analysis of the switching characteristics of a PRAM cell is performed with 2-dimensional transport simulation considering with band gap model. The behaviors of the basic I-V and key characteristic parameters are well described with the simulation. The scaling analysis on the electrical switching demonstrates that the threshold voltage increases as the bottom electrode is scaled down and it will be one of key concerns of future device scaling and development.

**Keywords**-PRAM; phase change; switching; snap-back; simulation.

## I. INTRODUCTION

The chalcogenide-based PRAM is one of the most promising next generation non-volatile semiconductor memories [1]. Even though it was introduced in 1960s, the physical understandings about the fundamental operational principles of the phase change cell are still lacking. Recently, Pirovano *et al.* reported an excellent investigation about electronic switching with the numerical simulation methodology [2]. However, the related governing principles of the electronic switching are more complicated compared to thermal and phase-change phenomena and more extensive analyses on the electronics switching are still required.

In this study, we set up the simulation environment with applying the bang-gap model of crystalline and amorphous GST and analyze the detailed switching mechanism [2]. In addition, the behavior of the switching threshold is studied with varying the temperature and doping in the GST. Finally, the dependence of threshold voltage on the bottom contact is analyzed with the impact on the scaling of the PRAM cell.

## II. SIMULATION METHODOLOGY

The simulation structure and circuit schematic are shown in Fig.1. A voltage source and a resistor are connected to the GST cell and the usual switching simulation of the amorphous GST is performed with the voltage boundary. The characteristics of crystalline and amorphous GST are defined with the band structure diagram as shown in Fig. 2. The Fermi level lies close to the valence band and the material conductivity is p-type. Crystalline state is described by the doping concentration as acceptor-like traps. The band structure of amorphous GST is characterized with well-known composition of three trap types; lone pairs located in the edge of the

valance band (trapping hole), acceptor-like trap ( $C_1^-$ ), and donor-like trap ( $C_3^+$ ) in vicinity of the valence band trap electrons [3]. These band models are implemented into the 2-dimensional drift-diffusion transport simulator; thus, the analysis for the realistic phase structures of the RESET state obtained from the thermal simulation is doable with current formulation.

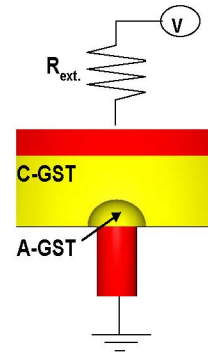


Fig. 1. Simulation and circuit schematic to analyze transition characteristics of GST material(amorphous/crystalline).

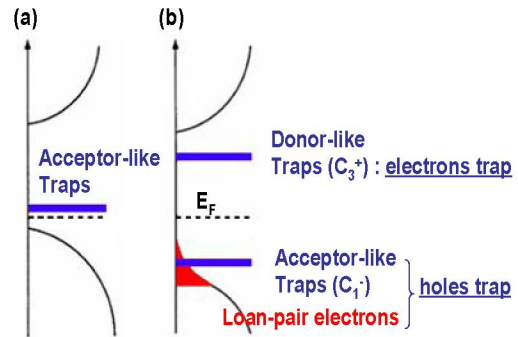


Fig. 2. Band diagrams of the amorphous and crystalline GST. (a) The presence of structural vacancies in the crystalline leading to acceptor-like traps (b) Structural defects generated by loan-pairs leading to donor/acceptor like defects.

## III. BASIC I-V CHARACTERISTICS

Fig.3 shows I-V characteristics of the GST cell at crystalline (SET) and amorphous (RESET) states. The simulation result describes the switching characteristics very well and is in a good agreement with measurement.

For the amorphous state, we indirectly analogize switching behaviors in on/off/negative states by monitoring the recombination rate obtained from simulation. The recombination rate depends on the electric field in the off-state as shown in Fig. 3 and 4. The recombination rate reaches the maximum at the threshold voltage and gradually decreases due to the avalanche generation. In the on-state, all trap sites are filled by carriers. As the generation rate rapidly increases, the high resistance state is changed into the low resistance one.

The holding voltage is defined as the minimum voltage needed to maintain the dynamic on-state after the occurrence of the threshold switching. It affects the reading and programming operations. As shown in Fig. 5, the holding voltage is independent of the external resistance ( $R_{ext}$ ). On the other hand, the holding current is sensitive to the external resistance. Fig. 6 shows a positive switching curve which is appeared in the case with larger external resistance than GST resistance.

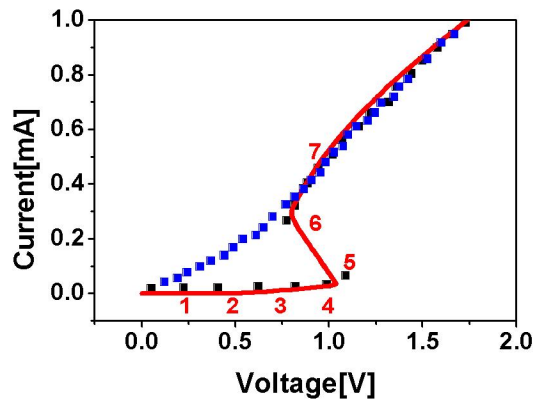


Fig. 3. I-V curves of amorphous and crystalline GST. Comparison with experimental(symbols) and simulation data(line)

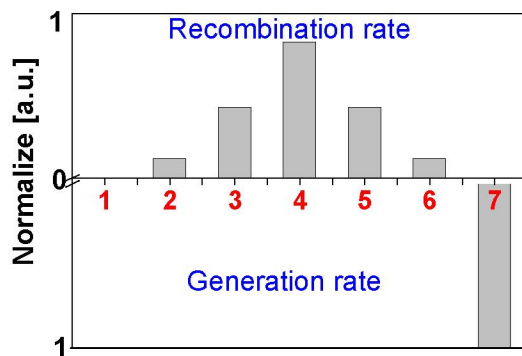


Fig. 4. Distribution of normalized recombination/generation rates at the off(1~4)/negative(5,6)/on-state(7) from the Fig.3.

#### IV. THRESHOLD VOLTAGE

We analyze the effects of temperature, doping, and bottom contact on the switching threshold voltage ( $V_{th}$ ). The dependence on the bottom contact size indicates the important scaling impact on electronic switching.

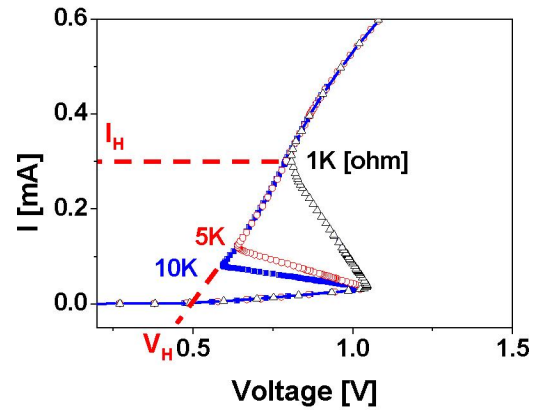


Fig. 5. Simulated holding voltage with varying external resistance (1K $\Omega$ , 5K $\Omega$  and 10K $\Omega$ ).

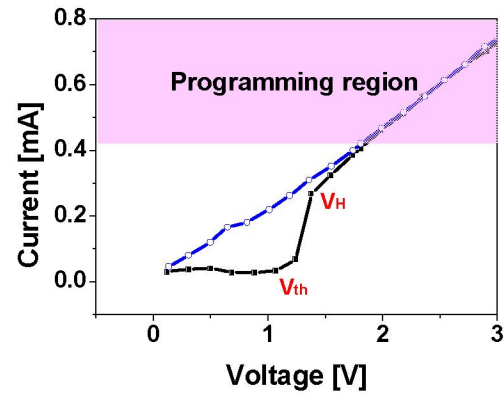


Fig. 6. Positive switching curve of amorphous GST due to higher external resistance than that of GST.

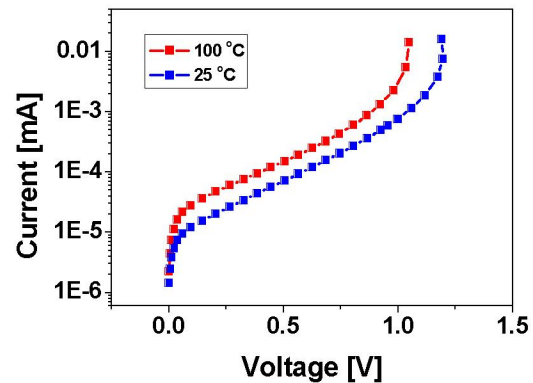


Fig. 7. Simulated I-V curve at both temperatures (20°C and 100°C)

### A. Temperature dependency

Fig. 7 shows the I-V characteristics of the amorphous state at the different temperature environments. Since impact ionization and carrier generation rate are a proportion to temperature, the threshold voltage slightly shifts to the lower voltage.

### B. Doping dependency

The doping process, such as the gas flow during the deposition process and sputtering, is a key step to improve device performance. For instance, the RESET current can be reduced significantly by incorporating the nitrogen into the GST. The effects of doping can be recognized with two kinds of impacts – the change of band gap due to lattice distortion and increase of the trap density [4,5]. In simulation, those effects related to GST doping are considered by modifying the band structure as described above. As shown in Fig. 8, increasing band gap results in the lower threshold voltage. In case of trap density, the opposite trend occurs. Since doping atoms destroy the twofold bonding of Te ( $2C^0 \rightarrow C_3^+ + C_1^-$ ), there are more lone-pairs electrons. This implies that more carriers are needed to be neutralized; therefore, the threshold voltage increases.

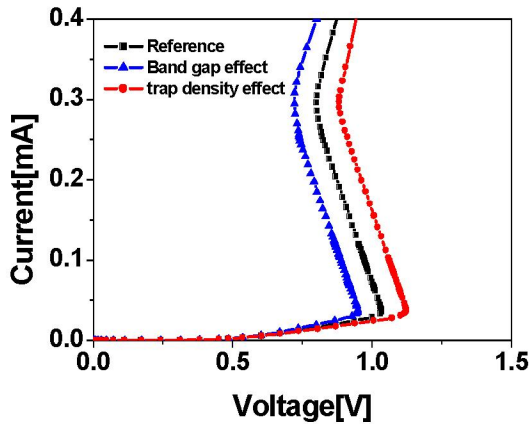


Fig. 8. Threshold voltage with changing doping condition; the shrinkage of band-gap by gas flow doping (triangles) and the increase of trap density by the sputter doping (circles).

### C. Effect of Bottom Contact Scaling

Fig. 9 shows that the threshold voltage increases as the volume of amorphous GST increases and saturates beyond the specific size. It clearly demonstrates that the excess RESET operation leads to a load of the SET operation. In addition, the effect of the bottom contact scaling is analyzed. The lateral size of the amorphous volume is set to be changed with bottom contact radius.

As shown in Fig. 10, the threshold voltage increases as the bottom contact is scaled down. One can verify this using the relation of threshold voltage and resistance[6]. With the smaller electrode, the potential drops between the bottom electrode and crystalline region increases as shown in Fig. 11.

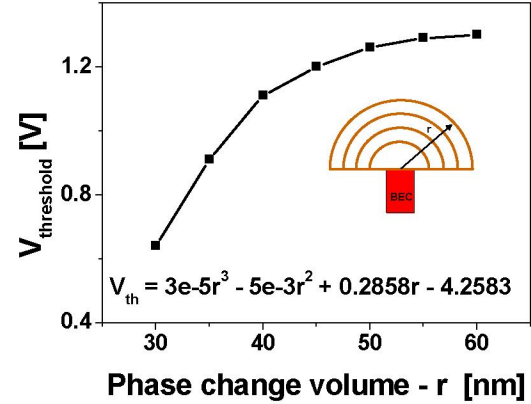


Fig. 9. Threshold voltage with changing amorphous volume size assuming the shape of hemisphere.

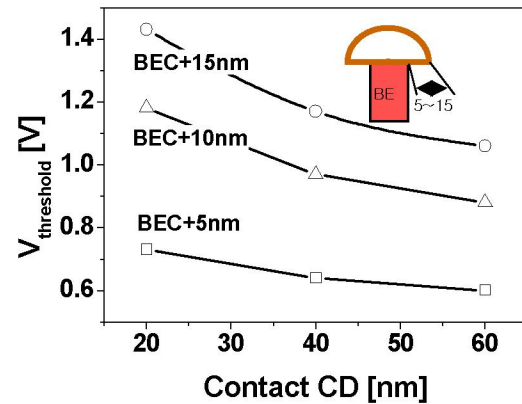


Fig.10. Electrode size dependency of threshold voltage. Amorphous size is assumed to be larger 5~15nm than that of electrode by 20~60nm.

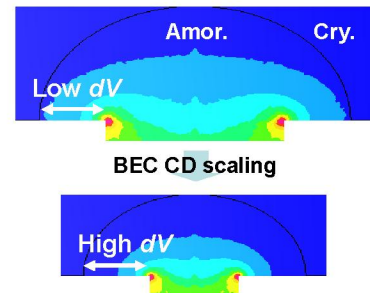


Fig. 11. As distribution of current density at different electrode size, threshold voltage is determined by the region of short current path. With the shrinkage of electrode size, the potential drop is more and more increasing.

## V. CONCLUSIONS

We have analyzed the switching characteristics of the PRAM cell by applying the 2-dimensional transport analysis with the band gap model. The behaviors of the basic I-V and key characteristic parameters are well described using simulation. Especially, the scaling analysis on the electrical switching demonstrates that the threshold voltage increases as the bottom electrode is scaled down and it will be one of key concern of the future device scaling and development.

## VI. REFERENCES

- [1] S. J. Ahn., Y.N. Hwang and Y.J. Song *et al.*, "Highly Reliable 50nm Contact Cell Technology for 256 Mb PRAM", Symp. VLSI Tech. Digest, pp. 88-89, 2005
- [2] A. pirovano A. Lacaita, A. Benvenuti and F. Pellizzer, "Electronic Switching in Phase Change Memories", IE EE Trans. Electr. Dev., Vol,51, pp. 452-459, 2004
- [3] D. Adler, M.S. Shur, M. Silver and S.R. Ovshinsky, "Threshold switching in chalcogenide glass thin films". J. Appl. Phys. Vol. 51, pp. 3289-3309, 1980.
- [4] T. H. Jeong, M.R. Kim, H.S. Seo, J.W. Park and C. Yeon, "Crystal Structure and Microstructure of Nitrogen-Doped Ge<sub>2</sub>Sb<sub>2</sub>Te<sub>5</sub> Thin Film, Jpn. J. Appl. Phys. Vol.39, pp. 2775-2779, 2000.
- [5] J. L. XIA, B.LIU, Z.T. SONG, S.L. FENG and B. C , "Electrical Properties of Ag doped Ge<sub>2</sub>Sb<sub>2</sub>Te<sub>5</sub> Films used for Phase Change Random Access Memory, Chin. Phys. Lett.. pp. 934-937, 2005.
- [6] D. Leardini, A. L. Lacaita, A. Pirovano, F. Pellizzer and R. Bez, "Analysis of Phase Distribution in Phase-Change Nonvolatile Memories", IEEE Elec. Dev. Lett. Vol, 25, NO. 7, pp. 507-509, 2004